Korean J. Chem. Eng., **25**(4), 744-753 (2008)

Filtration and regeneration behavior of polytetrafluoroethylene membrane for dusty gas treatment

Deqiang Jiang*, Weidong Zhang*,†, Junteng Liu, Wang Geng, and Zhongqi Ren***

*State Key Laboratory of Chemical Resource Engineering, Beijing University of Chemical Technology, Beijing 100029, P. R. China
**China Quality Certification Center, Beijing 100070, P. R. China
(*Received 23 March 2007 • accepted 4 December 2007*)

Abstract−With micron talcum particles and nano-$CaCO_3$ powder as test dust, a series of experiments have been carried out to systematically study the gas filtration and regeneration behavior of polytetrafluoroethylene membrane, and some comparisons were made with common filter media. The experimental results showed that the PTFE membrane had a filtration efficiency of above 99.99% for micron particles, and excellent regeneration behavior was obtained, though a much higher initial pressure drop existed. Based on the results, it was concluded that the PTFE membrane is an excellent surface-filtration media for micron particles. Effects of operation parameters, including airflow velocity, particle concentration and particle characteristics were also investigated. To better understand the evolution of pressure drop during the filtration process, a mathematical model with operation parameters and characteristics of particles was derived from the gas-solid two-phase flow theories. A novel method on the determination of regeneration period of the filter media was put forward based on the analysis of the pressure drop according to this model.

Key words: Polytetrafluoroethylene Membrane, Gas Filtration, Efficiency, Regeneration, Pressure Drop

INTRODUCTION

Particulate pollution caused by flue gases discharging from power plants and industrial combustion has become a serious environmental problem in many countries, especially those relying on coal as the main energy source[1]. Particulates suspended in the air have worsened the air quality and affected human health in most industrial cities [2]. Particulates less than 10 μm (PM_{10}) can easily penetrate the lungs into the alveoli and thus are more dangerous [3]. Therefore, it is becoming quite important to control or reduce the emissions of PM_{10}, and the development of efficient particulate collection technologies is necessary.

Gas filters are among the most widely used devices for particulate collection. The filter media is the key factor for the gas filtration process. Their structures and properties determine the application behavior of a filter. Flue gases always have high temperature and very complex chemical components, such as SO_2 and H_2S. Therefore, the filtration of flue gases has high demands on chemical and thermal stabilities of the filter media.

Ceramic is a typical filter media that has been successfully developed and applied to hot gas filtration. It has been widely recognized that ceramic filter is suitable for the filtration of high temperature and chemically aggressive process streams because of its excellent temperature and chemical resistance [4,5]. However, the applications of ceramic filter are usually limited to the rigidity and high cost of ceramic manufacture [6]. By the way, the durability of ceramic filter decreases resulting from the depth filtration [7]. Some novel methods, such as composite ceramic membrane [8], have been made to improve its economics, but these disadvantages are still quite difficult to overcome.

PTFE membrane is another typical gas filter media. It has been applied to the filtration of flue gases in power plants due to its excellent chemical and thermal stabilities [9,10]. PTFE has a narrower temperature range for hot gas filtration than ceramic, but it has an excellent elasticity and quite low adhesion and friction [11], so PTFE membrane filter membrane has more advantages in regeneration, maintenance and replacement of filter media. Application of PTFE membrane to gas filter will improve the economy of dust collection. However, few studies have been published on the behavior of PTFE membrane for gas filtration to guide the development of PTFE membrane filter.

Recently, Chinese researchers have successfully developed a novel process to produce PTFE membrane [12]. In order to apply the product to the filtration of flue gases, a plan on the systematic study of PTFE membrane filtration of flue gases has been arranged to get the basic data and guide the design of PTFE membrane filter. In this work, filtration efficiency, regeneration behavior of the PTFE membrane, factors affecting the pressure drop and the evolution of the pressure drop were investigated with micron talcum and nano-$CaCO_3$ powder as test dust at an ambient temperature of 20-25 °C.

Pressure drop is a primary factor for the design and operation of a filter, which reflects the level of resistance of a filter; also, it's the index that determines when to regenerate the filter media. During filtration, the total pressure drop mainly includes two parts: pressure drop through filter media and through cake layer. The former is determined by the structures and properties of the filter media. The latter is related to the structure and thickness of the cake layer loading on the filter, and it's the complex part due to the continuous growth and compression of the cake layer. Recent studies have mainly focused on characteristics of the cake layer, such as cake structure [13,14], cake formation [15], compression [16,17], and factors affect-

†To whom correspondence should be addressed.
E-mail: Zhangwd@mail.buct.edu.cn

ing pressure drop [18]. Some of them were based on computer programs [15,16], and the simulated results well agreed with experimental data. However, these computer models were so complex and abstract that they could not intuitively reflect the evolution of the pressure drop and effectively guide the industrial process. In this work, a mathematical model with operation parameters and characteristics of particles was derived from the gas-solid two-phase flow theories to better understand the evolution of the pressure drop during the filtration process. A novel method on the determination of the regeneration period of filter media was put forward based on the analysis of the pressure drop according to this model.

THEORY

Total pressure drop during filtration ΔP_t can be considered as the sum of the pressure drop through filter media ΔP_f and through dust cake ΔP_c. This sum can be written as:

$$\Delta P_t=\Delta P_f+\Delta P_c \tag{1}$$

1. Pressure Drop through Filter Media

The gas flow through the matrix of fiber media is considered as a viscous flow at a lower velocity. The pressure drop through filter media can be written as [19]:

$$\Delta P_f=\zeta_f \mu_g u_g \tag{2}$$

Where ζ_f is the resistance coefficient of clean filter media, which depends on the structure of the filter media, μ_g the viscosity of the gas, u_g the interfacial gas velocity through the membrane.

2. Pressure Drop through Dust Cake

The pressure drop through dust cake is the main part of total pressure drop during filtration. It is determined by the characteristics of the dust particles, the cake's properties and operation conditions. Traditional equations, such as Carman-Kozeny equation and Ergun Equation, can be used to describe the pressure drop. However, they were developed based on the assumption of monodisperse and spherical particles, and only used for some simplified cases. In fact, dust particles have irregular shapes and very wide particle size distributions. Recently, computer simulation has attracted many researchers, and some good results have been reported. However, these complex programs are not convenient to understand the evolution of the pressure drop through dust cake. In this work, a simple model will be developed based on traditional gas-solid two-phase flow theories. To classify the importance of those factors on the pressure drop and simplify the calculation process, we assume:

(1) The airflow velocity in this study is quite lower (0.009-0.022 $m \cdot s^{-1}$). The gas flow through micron interstices in the dust cake can be considered as laminar flow.

(2) During filtration process, the structure of dust cake is uniform. ε is used to represent the cake's porosity at t moment.

(3) Particle size distribution obeys the logarithm normal distribution as follows:

$$f(\ln d_P)=\frac{1}{\sqrt{2\pi}\ln\sigma_g}\exp\left[-\frac{(\ln d_P-\ln d_{Pm})^2}{2\ln^2\sigma_g}\right] \tag{3}$$

Where, d_{Pm} is the median diameter, $\ln\sigma_g$ the logarithm geometric standard deviation.

The cake layer loading on the membrane could be considered as a fixed-bed layer. The drag force on particles in unit volume of dust cake can be written by the cake's porosity and the gradient of pressure drop [20].

$$F_c=\varepsilon\frac{d(\Delta P_c)}{dh} \tag{4}$$

The height of the cake layer at t moment can be expressed with the following equation.

$$h=\frac{\eta u_g c_{P,i} t}{(1-\varepsilon)\rho_P} \tag{5}$$

Where, $c_{P,i}$ is the particle concentration at the inlet of the filter, η filtration efficiency, ρ_p the true density of the particles, t the filtration time.

F_c is also the sum of F_i, the drag forces acting on a single particle.

$$F_c=\int F_i f(\varepsilon) N_t f(d_P) d(d_P) \tag{6}$$

Where N_t is the number of particles in unit volume of dust cake, $f(\varepsilon)$ the void function.

F_i can be calculated by Eq. (7).

$$F_i=C_D\frac{1}{2}\rho_f u_i^2 A_P \kappa \tag{7}$$

Where, A_p is the projected area of a single particle in vertical direction, C_D the drag coefficient, u_i the interstitial gas velocity, ρ_f the gas density, κ the dynamic shape factor.

At the case of laminar flow, the drag coefficient can be written as:

$$C_D=\frac{24}{Re_P},\ \text{where } Re_P=\frac{d_P u_i \rho_f}{\mu} \tag{8}$$

Combining Eq. (6), (7) and (8), F_c can be derived.

$$F_c=3\pi\mu u_i k f(\varepsilon) N_t d_{Pm}\exp\left(\frac{1}{2}\ln^2\sigma_g\right) \tag{9}$$

From Eq. (10), N_t can be derived.

$$\varepsilon=1-\int\frac{\pi}{6}d_P^3 N_t f(d_P) d(d_P) \tag{10}$$

$$N_t=\frac{6}{\pi}(1-\varepsilon)\exp\left[-\left(3\ln d_{Pm}+\frac{9}{2}\ln^2\sigma_g\right)\right] \tag{11}$$

Combining Eq. (4), (5), (9), (11) and $u_i=u_g/\varepsilon$, then integrate, Eq. (12) can be derived.

$$\Delta P_c=18\mu u_g^2\eta c_{P,i}\frac{\kappa}{\rho_P d_{Pm}^2\exp(4\ln^2\sigma_g)}\frac{f(\varepsilon)}{\varepsilon^2}t \tag{12}$$

The affecting factors can be divided into three terms by Eq. (12). The first term represents the effect of operation parameters. The middle term indicates the effect of particle characteristics, and the last term means the effect of cake compression. Since the effect of σ_g on the pressure drop is an exponential term of $\exp(4\ln^2\sigma_g)$, and κ is always larger than 1, the effects of particle parameters cannot be neglected in the filtration of the particles with a broad size distribution.

Under certain conditions, the pressure drop through dust cake is greatly affected by cake compression. The evolution of cake com-

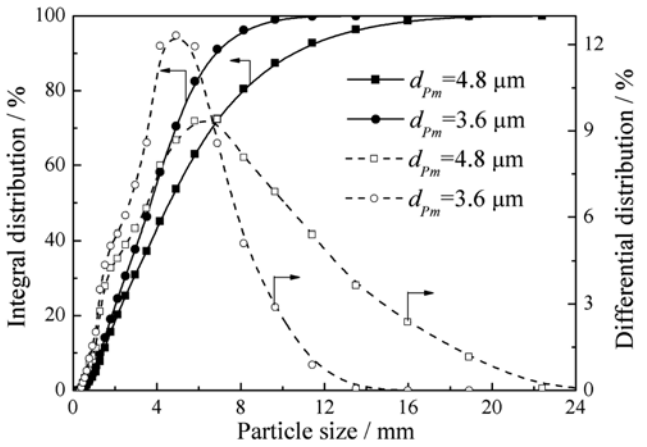

Fig. 1. Particle size distributions of the talcum powder used in this study.

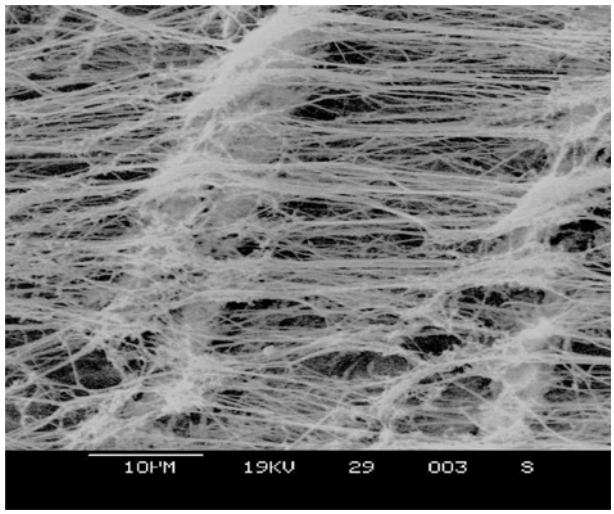

Fig. 2. SEM photograph of the PTFE membrane.

pression can be indicated by the void expression $f(\varepsilon)/\varepsilon^2$. The void function in Eq. (12) has to be determined by some special experiments [21], but it is a tough task. In this work, we will not discuss the absolute value of $f(\varepsilon)$. but indirectly estimate the value of the void expression $f(\varepsilon)/\varepsilon^2$ through our experimental data. Rearranging Eq. (12), the void expression can be written as:

$$\frac{f(\varepsilon)}{\varepsilon^2}=\frac{1}{18\mu u_g^2\eta c_{P,i}}\frac{\rho_P d_{Pm}^2 \exp(4\ln^2\sigma_g)}{\kappa}\frac{\Delta P_c}{t} \tag{13}$$

EXPERIMENTAL

1. The Powder

Two kinds of talcum powder were selected to simulate dusty air. Their particle size distributions are shown in Fig. 1. Besides, nano-$CaCO_3$ powder, provided by Research Center of the Ministry of Education for High Gravity Engineering and Technology in China, was used to measure the filtration efficiency of filter media. The average size of nano-$CaCO_3$ powder is about 30 nm. It's detailed properties and preparation are reported in reference [22]. Although the size of nano-$CaCO_3$ particles was in the range of nanometer, particles were easier to agglomerate due to the high surface energy of nano-particle. The conglomeration size was less than 3 μm, which is little smaller than talcum particles. All powders were dried for 12 h prior to use in order to avoid the problems of particle agglomeration and adhesion.

2. The Filter Media

Polytetrafluoroethylene (PTFE) membrane was used as filter media. It was provided by China Quartermaster Research Institute of the General Logistic Dept of CPLA. The membrane has a thickness of 39.5 μm and a porosity of 76.4%, and its surface tension is 0.019 $N\cdot m^{-1}$. Fig. 2 shows an SEM photograph of the PTFE membrane, from which irregular pores and the 3-dimension structure can be observed.

In addition, PP Needle Felt, a common filter medium widely applied to dust collection, was used to compare the filtration behavior with PTFE membrane. It was purchased from Jiangsu Dongfang filter bag limited company (China). It has a thickness of 1.8 mm and a weight of 550 $g\cdot m^{-2}$, and its surface tension is 0.031 $N\cdot m^{-1}$, which is over 1.6 times as that of PTFE membrane.

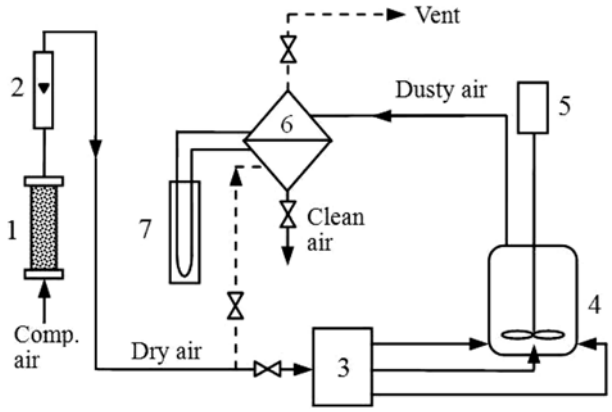

Fig. 3. Schematic diagram of the experimental set-up.

1. Silica-gel drier
2. Gas rotameter
3. Gas splitter
4. Dust generator
5. Motor stirrer
6. Membrane filter
7. Water manometer

3. Experiment Procedure

A schematic diagram of the experimental set-up is shown in Fig. 3. The compressed dry air was used to create dusty test air. The flow velocity could be controlled by a gas rotameter and was kept constant in the whole filtration process. Firstly, dry air was divided into three streams through a gas splitter, and then the three streams flowed into the dust generator from its bottom in three symmetric directions. In the generator, the dust bed was fluidized by the airflow and stirrer. Then, dusty air was created and flowed into the upper part of the membrane filter. On the surface of PTFE membrane, the dust particles were captured.

The membrane filter was specially designed. It was constituted by two symmetrical parts with horn shape. Both of the inlet and outlet were horn mouths with gradually changing cross section diameter to reduce the friction resistance and avoid the particles from adhering to the wall of the filter. PTFE membrane was set in the middle of the filter and supported by a nylon meshwork. The effec-

tive membrane area was 314.2 cm^2.

The method of regenerating filter media used in the study was reverse flow with clean air. The dashed lines in Fig. 3 are the regenerating path. In the regenerating process, the airflow velocity was 0.031 $m \cdot s^{-1}$, which was higher than that in filtration process to effectively remove the dust cake. It only took a very short time to regenerate because of the slippery surface of PTFE membrane. The reverse flow time was determined to be 30 seconds in this study.

Pressure drop through the filter was measured by a water manometer. Particle concentration at the inlet of the filter was determined by the weight decrement of particles in the generator at corresponding time (Eq. (14)). All experiments were carried out under ambient temperature of 20-25 ºC.

$$c_{P,i} = \frac{M_0 - M_t}{Qt} \tag{14}$$

Where, M_0 is the weight of dust regenerator before filtration, M_t the weight of dust regenerator at t moment, Q the air flux.

4. Measurement of Filtration Efficiency

Generally, filtration efficiency was tested by weighing the mass of particles escaping from the filter or measuring the particle concentration at the inlet and outlet with optical apparatus. The accuracy of the former method is very poor, so it cannot be applied in the case of high filtration efficiency. The latter is a widely used method with a very high accuracy, but the measuring range of its probe head is very limited. In our study, the particle concentration at the inlet of the filter was relatively high and the concentration at the outlet was very low, so simultaneous measurements of the concentrations at the inlet and outlet could not be carried out by the above methods. Thus, a novel method was developed to test the particle concentration at the outlet in this work.

$$CaCO_3 + HCl = CaCl_2 + H_2O + CO_2\uparrow \tag{I}$$

$$Ca^{2+} + Y^{4-} = CaY^{2-} \tag{II}$$

As seen as from chemical formulas (I) and (II), the principle of the new method is chemical absorption of $CaCO_3$ in HCl solution, then titration of Ca^{2+} using 0.1 $mol \cdot L^{-1}$ EDTA(H_4Y) standard solution. Nano-$CaCO_3$ particles were selected to test the filtration efficiency based on two reasons: (a) the particles can be fast absorbed in the strong acid solution; (b) since the size of nano-$CaCO_3$ particles was a little smaller than talcum particles, the resulting measured with nano-$CaCO_3$ particles would more persuasively reflect the filtration efficiency of PTFE membrane. Measuring accuracy of the method was 10 ppm for Ca^{2+} concentration. The absorption setup is shown in Fig. 4.

The particle concentration at the outlet and filtration efficiency can be calculated from Eq. (15) and (16), respectively.

$$c_{P,o} = \frac{C_{Ca^{2+}} V_{HCl} M_{CaCO_3}}{Qt} = \frac{C_{EDTA} V_{EDTA} M_{CaCO_3}}{Qt} \tag{15}$$

$$\eta = \frac{c_{P,i} - c_{P,o}}{c_{P,i}} \tag{16}$$

Where, $c_{P,o}$ is the particle concentration at the outlet of the filter, $C_{Ca^{2+}}$ the Ca^{2+} concentration in the absorbed solution, V_{HCl} the volume of the absorbed solution, M_{CaCO_3} the molar mass of $CaCO_3$, C_{EDTA} the concentration of EDTA standard solution, V_{EDTA} the volume of EDTA standard solution used to titrate the absorbed solution.

RESULTS AND DISCUSSION

1. Pressure Drop through the Membrane

Prior to the study of the filtration behavior of PTFE membrane, pressure drop through the filters for clean air was tested. The experimental results are shown in Fig. 5. The fitted lines show that the pressure drop is proportional to the airflow velocity for PTFE membrane and Needle Felt, and the pressure drop through PTFE membrane is much higher than that through Needle Felt.

According to Eq. (2), resistance coefficients (20 ºC) of the filter media can be estimated from the slope of pressure drop versus flow velocity line. The calculated results of resistance coefficient are 4.90×10^9 m^{-1} for PTFE membrane and 3.80×10^8 m^{-1} for Needle Felt, respectively. The former is over ten times higher than the latter because PTFE membrane has smaller pore size and denser structure than Needle Felt. It can be predicted from the results that a higher initial pressure drop will occur during filtration with PTFE membrane filter.

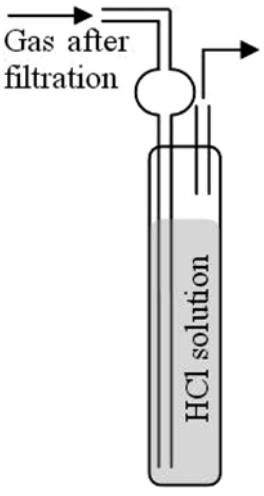

Fig. 4. Schematic diagram of the absorption setup.

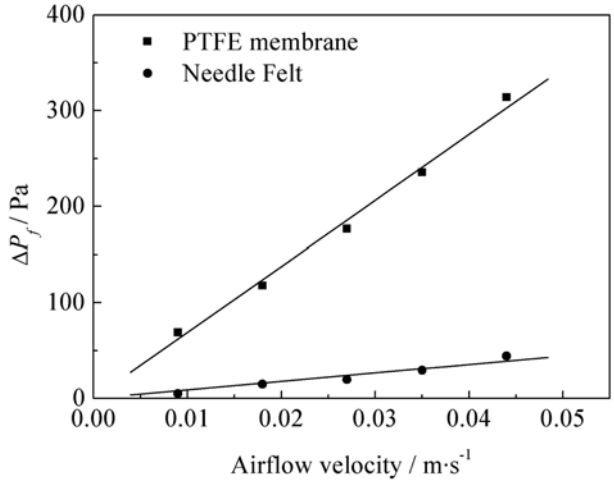

Fig. 5. Pressure drop through the filter media as a function of the airflow velocity.

Table 1. Comparison of the filtration efficiencies of PTFE membrane and Needle Felt

Filter media	Filtration time/min	Particle concentration/ $g \cdot cm^{-3}$		Filtration efficiency/%
		Inlet	Outlet	
PTFE membrane	30	4.67	undetected	>99.99
	45	4.62	undetected	>99.99
	60	4.67	undetected	>99.99
Needle felt	60	3.56	0.14	96.07
	60	3.87	0.07	98.09
	60	3.40	0.07	97.82

2. Filtration Efficiency

The filtration efficiency of these two filter media were tested by chemical absorption of $CaCO_3$ and titration of Ca^{2+} using 0.1 $mol \cdot L^{-1}$ EDTA solution. Experimental results are presented in Table 1.

For the filtration of PTFE membrane, no Ca^{2+} is detected in the absorption solution. It means the concentration of Ca^{2+} is lower than the accuracy of the analytical method (10 ppm of Ca^{2+}). In the case, corresponding filtration efficiency is higher than 99.99%. While Needle Felt is used as filter media, the filtration efficiency is 96%-98%, which shows some nano-$CaCO_3$ particles discharge from the outlet of Needle Felt filter.

The differences of filtration efficiency between PTFE membrane and Needle Felt are related to the structures of the filter media. For PTFE membrane, the pore size is micron and irregular (Fig. 2), and its distribution can be controlled in a narrow variation band. Thus, almost all particles can be captured by PTFE membrane. For Needle Felt, its pore size is bigger than that of PTFE membrane. Some fine particles could enter into the inner matrix of Needle Felt. With the continuous flow of air streams, these particles are brought out of the filter from the inner part of Needle Felt. Therefore, the filtration efficiency of Needle Felt is lower than that of PTFE membrane. However, after several minutes, particles form a bridge across the inner pores. Then, the bridge improves the filtration efficiency.

The above results indicate PTFE membrane had a higher filtration efficiency of almost 100% for micron particles. It will better satisfy the progressively strict standard of environmental protection than traditional filter media like Needle Felt.

3. Regeneration Behavior of the Membrane

In order to study the regeneration behavior of PTFE membrane, continuous filtration-generation experiments were carried out at high particle concentration of 17.40 $g \cdot m^{-3}$ using micron talcum particles of d_{Pm}=4.8 mm. The flow rate was 0.022 $m \cdot s^{-1}$ during filtration and 0.031 $m \cdot s^{-1}$ during regeneration by reverse flow, and the reverse flow time was 30 s in all experiments.

3-1. The Case of Fixed Maximum Pressure Drop

In this case, the maximum of pressure drop was fixed at 1 kPa in each cycle. Filtration process will be stopped and regeneration process starts when the pressure drop rises to 1 kPa. Experimental results are shown in Fig. 6. The curves indicate the evolution of the pressure drop through PTFE membrane filter and Needle Felt filter during several filtration-generation cycles. In the first cycle, the pressure drop of Need Felt filter increases slowly due to the lower initial pressure drop and lower filtration efficiency. It takes more time to reach the maximum than the PTFE membrane filter. With the experiments going on, the durations are shorter and shorter, and the duration decreases seriously from 20 min in the beginning to 3 min

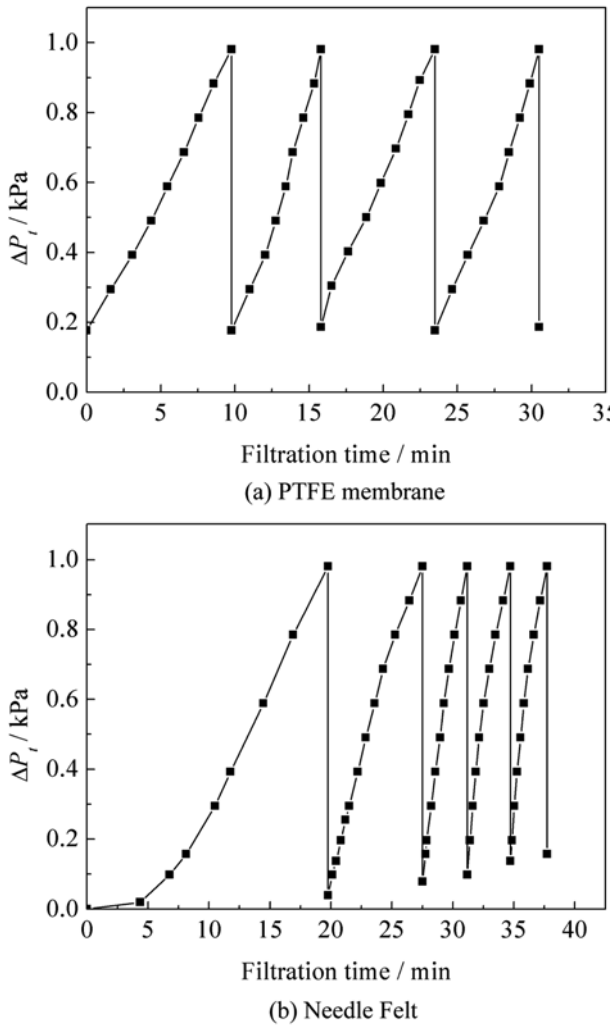

Fig. 6. Evolution of the pressure drop at the case of fixed maximum pressure drop.

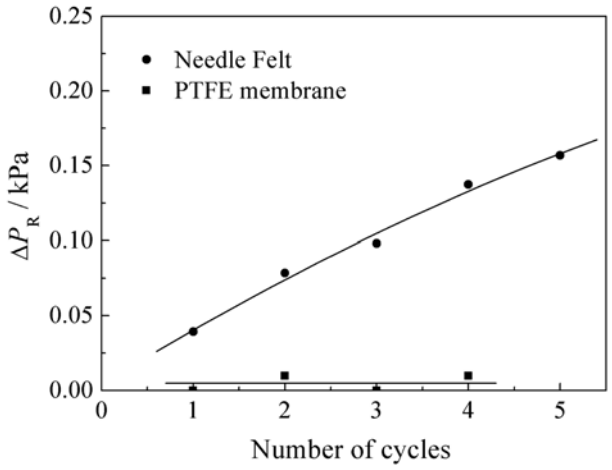

Fig. 7. Evolution of the residual pressure drop.

after 5 cycles.

A significant difference of residual pressure drop can be observed between Needle Felt filter and PTFE membrane filter from Fig. 7. The residual pressure drop of Needle Felt filter increases sharply as the cycle progresses, while for PTFE membrane filter, the residual pressure drop is almost zero after reverse flow in each cycle.

Above differences are mainly caused by two factors, material properties and structures of the filter media. During the filtration process, almost all of the dust particles are captured on the surface of PTFE membrane because of its micron pores. The particles can easily fall off from the surface. Furthermore, PTFE membrane has a quite low interfacial tension, only 0.019 N/m, which means the adhesion forces between PTFE membrane and dust particles are very small. No particle can be adhered on its surface with the continuous reverse flow. Therefore, PTFE membrane can be cleaned very thoroughly and almost no residual pressure drop exists.

Compared with PTFE membrane, Needle Felt has a rough surface and big pore size. Many particles are adhered to the fiber in the inner matrix or on the surface of Needle Felt. After 30 s reverse flow cleaning, the particles could not be removed completely due to the adhesion force and interception of the fibers. As the filtration-regeneration cycles progressed, more and more particles remained on the surface or in the inner part of Needle Felt, more and more pores of Needle Felt are clogged. Accordingly, the residual pressure drop of Needle Felt greatly rises and the duration sharply decreases.

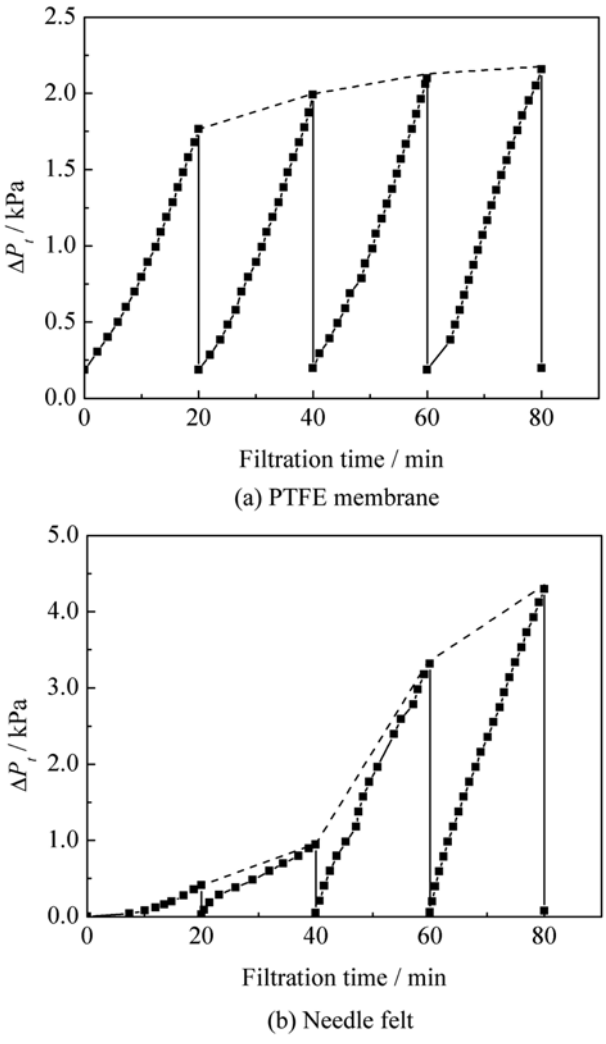

Fig. 8. Evolution of the pressure drop at the case of fixed filtration period.

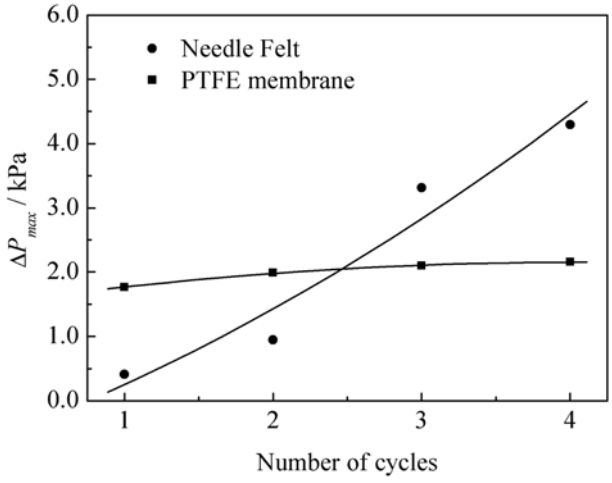

Fig. 9. Evolution of the maximum pressure drop.

3-2. The Case of Fixed Filtration Period

To further investigate the regeneration behavior of PTFE membrane, experiments were carried out for the case that the filtration period was fixed at 20 min. The results are shown in Fig. 8.

Due to the higher initial pressure drop and filtration efficiency of PTFE membrane, the pressure drop of PTFE membrane filter is greater than that of Needle Felt filter in the first cycle. However, as cycles progress, the maximum of the pressure drop in each cycle increases sharply for Needle Felt filter. The reason should be that the pores of filter media are gradually clogged and they cannot be recovered by reverse flow. During the third cycle, the maximum pressure drop has far exceeded the value that PTFE membrane filter reaches (Fig. 9). As seen from Fig. 9, the maximum changes very little for PTFE membrane, only from 1.8 kPa to 2.1 kPa after 4 cycles, while 0.4 kPa to 4.3 kPa for Needle Felt. These also indicate that PTFE membrane can get a quick and complete recovery, while Needle Felt is worsened due to the particle clogging.

Above results and discussion on the filtration efficiency and regeneration behavior show that PTFE membrane is a surface-filtration media for micron particles, whereas depth-filtration occurs while using Needle Felt as filter media. The excellent regeneration behavior also indicates PTFE membrane has a longer life span and needs a lower frequency of regeneration than Needle Felt.

4. Influence of Operation Parameters on the Pressure Drop of PTFE Membrane Filter

4-1. Influence of Airflow Velocity

Influence of airflow velocity on the pressure drop was tested in the range 0.009 to 0.022 $m \cdot s^{-1}$ at particle concentration of 5.14 $g \cdot m^{-3}$ by using micron talcum particles of d_{Pm}=4.8 μm. The results are plotted in Fig. 10. As can be seen, the pressure drop is greater at higher airflow velocity, and the pressure drop increases more drastically at higher airflow velocity. According to Eq. (7), airflow velocity has a significant effect on the drag force acting on a single particle, and the relationship between airflow velocity and the drag force

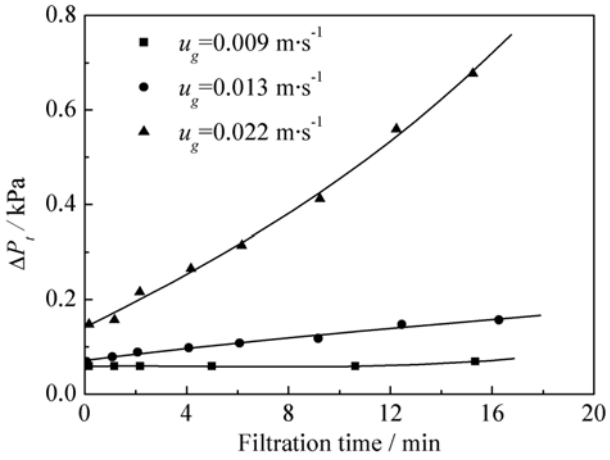

Fig. 10. Evolution of the pressure drop at different airflow velocities.

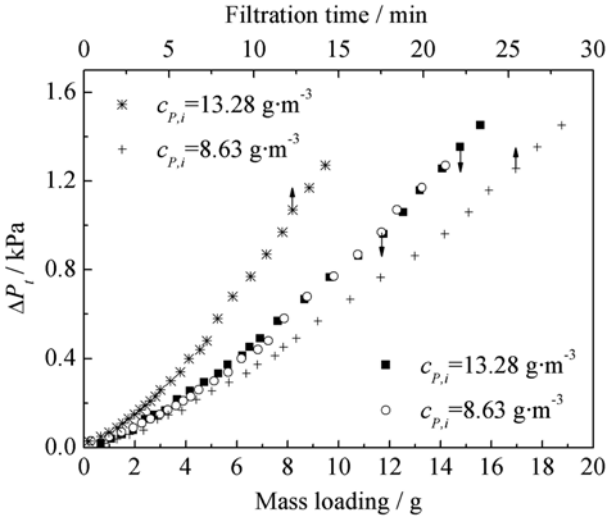

Fig. 11. Evolution of the pressure drop at different particle concentrations.

on a particle is quadratic. Therefore, the higher the airflow velocity, the larger pressure drop occurs. The effect of airflow velocity also can be analyzed based on Eq. (12). Besides, the higher airflow velocity makes the dust cake more packed due to the stronger drag force, which brings about a more significant increasing trend of the pressure drop.

4-2. Influence of Particle Concentration

To investigate the effect of particle concentration, a series of experiments were carried out by varying the inlet concentration at the flow velocity of 0.022 m·s^{-1} by using micron talcum particles of d_{Pm}=4.8 μm. As can be seen from Fig. 11, the pressure drop when $c_{p,i}$=13.28 g·m^{-3} is much higher than that when $c_{p,i}$=8.63 g·m^{-3}. The phenomenon is very easy to understand from the fact that more particles loaded on the surface of PTFE membrane at the higher particle concentration within the same time. However, it cannot be confirmed that the difference of particle concentration is the only factor. Whether the packed patterns of the dust cake also change with the concentration increasing, further analysis is necessary. The curves

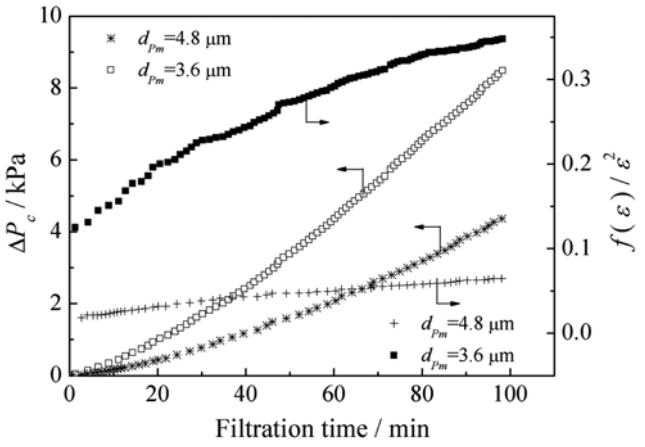

Fig. 12. Evolution of the pressure drop and the void expression for different particles.

of pressure drop vs. mass loading of dust are plotted in Fig. 11. It's observed that the trends of two curves are almost identical. That indicates the pressure drops are identical at the same mass loading of particles. It also means the cake's density should be the same at a certain mass loading of particles, and the particle concentration does not affect the pressure drop by changing the cake's structure. The result is not similar to the work of Song et al. [23], who considered that particle concentration can cause changes in the deposited pattern of particles in a high mass loading range. Nevertheless, the airflow velocity and filtration media are quite different between this work and Song's. As discussed above, they have significant effects on the pressure drop.

4-3. Influence of Particle Characteristics

Influence of particle characteristics on the pressure drop was tested at the flow velocity of 0.022 m·s^{-1} and particle concentration of 8.63 g·m^{-3}. Evolution of the pressure drop when d_{Pm}=3.6 and 4.8 μm particles is shown in Fig. 12. The curves clearly show that the pressure drop is lower for bigger particles. The result agrees with Eq. (12) where the pressure drop is inversely proportional to the square of the particle diameter. According to Eq. (10), the drag force is greater as N_t is higher. There are more particles in unit volume of dust cake for the smaller particles. Furthermore, the smaller particles have larger specific area, which leads to a stronger friction force between the particles and airflow. Therefore, the pressure drop is higher during collecting small particles.

The polydispersity of the particles is another factor affecting the pressure drop. The value of $\ln\sigma_g$ stands for the polydispersity of the particles. $\ln\sigma_g$=0.76 for d_{Pm}=4.8 μm particles, and 0.66 for d_{Pm}=3.6 μm particles. This indicates that the particles of d_{Pm}=4.8 μm have a wider size distribution than d_{Pm}=3.6 μm particles, which also can be seen from the Fig. 1. It's quite difficult to investigate the effect of the polydispersity as a single factor, but the combined influence of the particle size and polydispersity can be reflected by the void expression $f(\varepsilon)/\varepsilon^2$ according to Eq. (13). The calculated results are plotted in Fig. 12. Seen from that, the value of $f(\varepsilon)/\varepsilon^2$ for d_{Pm}=3.6 μm particles is higher than that of d_{Pm}=4.8 μm particles, and the increase in the value of $f(\varepsilon)/\varepsilon^2$ is more obvious for d_{Pm}=3.6 μm particles, which indicates that the particle size and polydispersity have a common effect on the pattern of the cake layer.

5. Analysis on Evolution of the Pressure Drop

The filtration process of PTFE membrane can be divided into three stages: surface-filtration, transition stage and cake-filtration. Due to the relatively high particle concentration, membrane surface is completely covered by the particles in no more than 30 s just after the filtration start, and the process quickly changes from surface-filtration to cake-filtration at the beginning of the experiments. Therefore, the duration of surface-filtration and transition stage can be neglected compared to the whole process. Besides, there is almost no clog in the inner part of PTFE membrane because it's a surface filter media. The dust cake only forms on the membrane surface. So evolution of the pressure drop can be considered to be totally resulting from the deposition of the particles on the surface of PTFE membrane. In the following paragraphs, the pressure drop through dust cake will be analyzed based on the data in Fig. 12.

The pressure drop through dust cake can be calculated by Eq. (1), where the pressure drop through PTFE membrane equals the corresponding data in Fig. 5. To clearly describe the evolution of pressure drop at the beginning, the initial section of the curves in Fig. 12 is magnified. The result is shown in Fig. 13. It can be observed that the pressure drop increases linearly in the first 10 minutes. The linear trend indicates that there is no change of cake's porosity according to Eq. (12), and the trend is caused by the increase in the cake's thickness. Along with the initial linear trend, two lines are drawn in Fig. 13. The line represents the evolution of the pressure drop through dust cake without cake compression. Extrapolating the line to the whole time range, a deviation can be noticed in Fig. 14, and it's more and more obvious with the filtration time. The deviation shows that the dust cake is continuously compressed during the growth of dust cake. According to the line, the pressure drop through dust cake, ΔP_c, can be divided into two parts: the pressure drop ΔP_{cL} brought about by the cake's thickness at the initial cake porosity and $\Delta P_{c\varepsilon}$ resulting from the cake's compression. ΔP_{cL} can be obtained by the experimental data, also expressed by Eq. (12) as Eq. (17). $\Delta P_{c\varepsilon}$ can be calculated by ΔP_c minus ΔP_{cL}.

$$\Delta P_{cL} = 18\mu u_g^2 \eta c_{P,i} \frac{\kappa}{\rho_P d_{pm}^2 \exp(4\ln^2\sigma_g)} \frac{f(\varepsilon_0)}{\varepsilon_0^2} t = kt \quad (17)$$

Where, ε_0 is the initial cake porosity, k the slope of the line in Fig. 14, k=0.036 and 0.016 for d_{Pm}=3.6 μm and d_{Pm}=4.8 μm particles, respectively.

In order to study the importance of the two factors, the values of $\Delta P_{cL}/\Delta P_c$ and $\Delta P_{c\varepsilon}/\Delta P_c$ are plotted in Fig. 15. From the curves, it can be found that the proportion of $\Delta P_{c\varepsilon}$ in ΔP_c gradually increases with the filtration time, while the value of $\Delta P_{cL}/\Delta P_c$ decreases. After about one hour, the value of $\Delta P_{c\varepsilon}/\Delta P_c$ rises to more than one half of ΔP_c, and $\Delta P_{c\varepsilon}$ dominates the pressure drop. The phenomena also indicate a strong compression happened in the dust cake. The cake's porosity had a much greater effect on the pressure drop than the cake's thickness.

The point of $\Delta P_{cL}/\Delta P_c$=0.5 or $\Delta P_{c\varepsilon}/\Delta P_c$=0.5 is marked by t_m, which divides the whole range into two sections. In the first section, the pressure drop is lower and ΔP_{cL} is the dominant part. In the second one, the pressure drop is higher and dominated by $\Delta P_{c\varepsilon}$. The pressure drop reflects the resistance level of a filter. The operation in the second section will need more power. Therefore, timely regenerating the filter media is necessary to reduce the energy consumption. In the industrial process, the regeneration period is determined

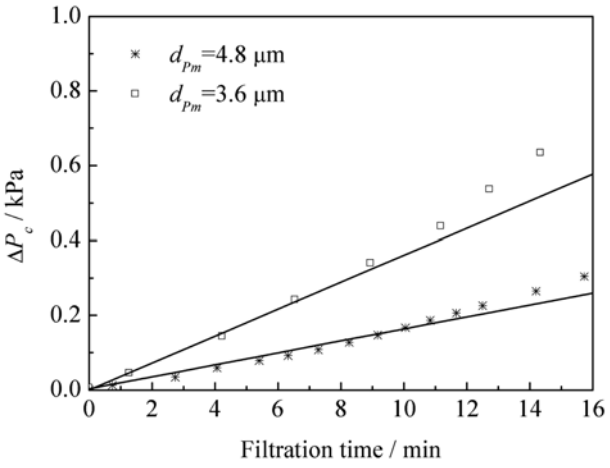

Fig. 13. The initial evolution of the pressure drop in Fig. 12.

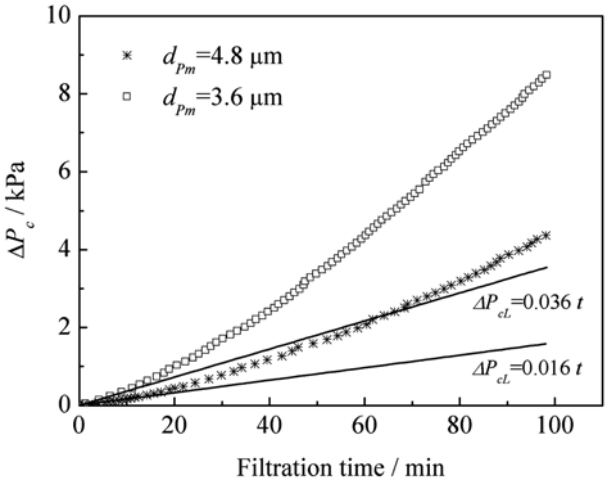

Fig. 14. Deviations of the experimental data from extrapolation of the initial trend.

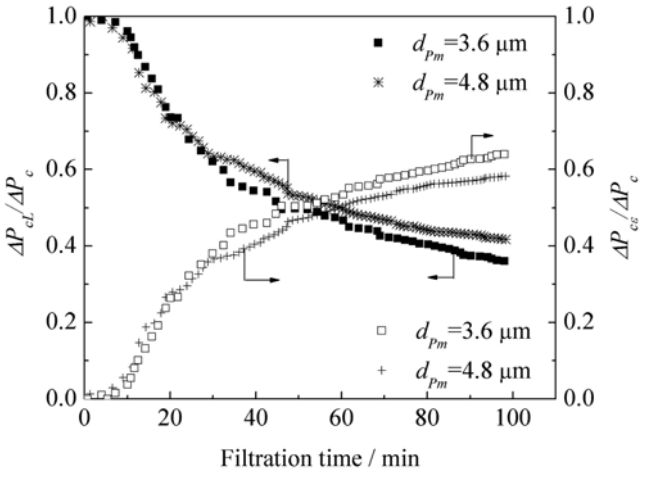

Fig. 15. Variations of the ratios ($\Delta P_{cL}/\Delta P_c$ and $\Delta P_{c\varepsilon}/\Delta P_c$) with filtration time.

by a limited pressure drop (ΔP_{Lim}). Once the pressure drop exceeds ΔP_{Lim}, regeneration will begin. However, it may not be economic if the time that the pressure drop rises to ΔP_{Lim} is located in the range of $\Delta P_{c\varepsilon}/\Delta P_c>0.5$ according to the above discussion. The following relationships should be satisfied to make sure that regeneration starts in the first section.

$$\Delta P_{cL}/\Delta P_{Lim}\leq 0.5 \tag{18}$$

$$\text{And } \Delta P_{c\varepsilon}/\Delta P_{Lim}\leq 0.5 \tag{19}$$

Eq. (19) is the same as

$$t_R\leq t_m \tag{20}$$

Through Eq. (17) and (19), the following expression can be derived.

$$t_R\leq \Delta P_{Lim}\frac{1}{36\mu u_g^2\eta c_{P,i}}\frac{\rho_P d_{Pm}^2\exp(4\ln^2\sigma_g)}{\kappa}\frac{\varepsilon_0^2}{f(\varepsilon_0)} \tag{21}$$

Combining Eq. (20) and (21), the latest time when to start regeneration during a filtration process can be calculated. Based on Eq. (21), the latest time is determined by many factors including operation conditions, filtration efficiency, particle characteristics and the initial cake porosity under a certain limited pressure drop. Since the void function $f(\varepsilon)$ and the initial cake porosity are unknown, t_R cannot be directly calculated by Eq. (21). But the value of the expression $[1/(36\mu u_g^2\eta c_{P,i})]/[\rho_P d_{Pm}^2\exp(4\ln^2\sigma_g)/\kappa]/[\varepsilon_0^2/(f(\varepsilon_0)]$ can be calculated with the slope k according to Eq. (17).

For the cases discussed in these paragraphs, t_m is 46.0 and 57.4 min for d_{Pm}=3.6 μm and d_{Pm}=4.8 μm particles, respectively. t_R can be determined by Eqs. (20) and (21) if a limited pressure drop is given. The calculated results are shown in Table 2. These data indicate that the time is earlier for the filtration of d_{Pm}=3.6 μm particles than for the filtration of d_{Pm}=4.8 μm particles. The reason may be that the particle size and polydispersity have a common effect on the pattern of the cake layer.

Above calculations are all based on the experimental data. Although the calculation process seems to be relatively complex, the results can well guide our work. However, the determination of the regeneration period of filter media needs a prediction equation for the applications to the industrial dust removal. Therefore, future work is necessary to acquire a detailed expression of the void function $f(\varepsilon)$ and the law of the initial cake porosity under different operation conditions.

CONCLUSIONS

A systematic study on the gas filtration and regeneration behavior of PTFE membrane with micron particles has been carried out. Compared with Needle Felt, a common filter medium, PTFE membrane has a denser structure, which brings about a higher initial pressure drop and much higher filtration efficiency, above 99.99% for nano-$CaCO_3$ particles. Therefore, the PTFE membrane will better meet environmental requirements for the collection of PM_{10}. Regeneration behavior of PTFE membrane was discussed in detail. The experimental results show that PTFE membrane can be almost completely regenerated in each cycle just through 30 s reverse flow. It means the regeneration frequency would be reduced and the lifespan prolonged if PTFE membrane were used as the filter media. According to the analysis of the filtration efficiency and regeneration behaviors, a conclusion is made that PTFE is an excellent surface-filtration filter media.

Moreover, the effects of operating parameters were investigated in this study. Higher airflow velocity could bring about a stronger drag force, which causes a rapid increase in the pressure drop. Particle concentration has an effect on the velocity of particle deposit on the membrane surface, but no effect on the cake's porosity. The particle size and polydispersity have a significant effect on the pattern of the cake layer, and smaller particles and narrower size distribution were found to entail a lower pressure drop. To better understand the evolution of the pressure drop, a model with operation parameters and characteristics of particles was derived from the gas-solid two-phase flow theories, and the evolution of the pressure drop was analyzed in detail by the model. Finally, a novel method on the determination of the regeneration period of filter media was put forward based on the analysis of the pressure drop according to the model, but the method needs to be perfected because the void function is unknown. Future work is necessary to acquire the detailed expression of void function $f(\varepsilon)$ and the law of the initial cake porosity under different operation conditions.

Table 2. The calculated results of regeneration period for the cases in Fig. 12

ΔP_{Lim}/kPa	t_R≤/min	
	d_{Pm}=3.6 μm	d_{Pm}=4.8 μm
0.5	6.9	15.6
1.0	13.9	31.3
2.0	27.8	57.4

ACKNOWLEDGMENTS

This work was supported by the High Technology Research and Development Program ("863" Program) of China (No. 2002AA649280).

NOMENCLATURE

A_p : projected area of a single particle in vertical direction [m^2]
C_D : drag coefficient
$c_{P,i}$: particle concentration at the inlet of the filter [$kg\cdot m^{-3}$]
$c_{P,o}$: particle concentration at the outlet of the filter [$kg\cdot m^{-3}$]
$C_{Ca^{2+}}$: Ca^{2+} concentration in the absorbed solution [$mol\cdot L^{-1}$]
C_{EDTA} : concentration of EDTA standard solution [$mol\cdot L^{-1}$]
d_{Pm} : median diameter [m]
F_c : drag force acting on particles in unit volume of dust cake [$N\cdot m^{-3}$]
F_i : drag force acting on a single particle [$N\cdot m^{-3}$]
h : height of cake layer [m]
k : line slope
M_{CaCO_3} : molar mass of $CaCO_3$ [$g\cdot mol^{-1}$]
N_t : number of particles in unit volume of dust cake
t : filtration time [s]
t_m : filtration time at $\Delta P_{cL}/\Delta P_c$=0.5 [min]
t_R : time when to start regeneration the filter media [min]
u_g : interfacial gas velocity [$m\cdot s^{-1}$]
u_i : interstitial gas velocity [$m\cdot s^{-1}$]

V_{EDTA} : volume of EDTA standard solution used to titrate the absorbed solution [L]
V_{HCl} : volume of the absorbed solution [L]
ΔP_c : pressure drop through dust cake [Pa]
ΔP_f : pressure drop through filter media [Pa]
ΔP_t : total pressure drop during filtration [Pa]
ΔP_{Lim} : limited pressure drop [Pa]
ε : cake's porosity
ε_0 : initial cake porosity
ζ_f : resistance coefficient of clean filter media [m^{-1}]
η : filtration efficiency
κ : dynamic shape factor
μ_g : viscosity of the gas [Pa·s]
ρ_f : gas density [$kg \cdot m^{-3}$]
ρ_p : true density of the particles [$kg \cdot m^{-3}$]
σ_g : geometric standard deviation

REFERENCES

1. Y. Zhao, S. Wang, K. Aunan, H. M. Seip and J. Hao, *Sci. Total. Environ.*, **366**, 500 (2006).
2. E. Petavratzi, S. Kingman and I. Lowndes, *Miner. Eng.*, **18**, 1183 (2005).
3. R. M. Harrison and J. Yin, *Sci. Total. Environ.*, **249**, 85 (2000).
4. S. Heidenrelch and B. Schelbner, *Filtr. Separat.*, **May**, 22 (2002).
5. J. D. Chung, T. W. Hwang and S. J. Park, *Korean J. Chem. Eng.*, **20**, 1118 (2003).
6. M. Theodore J, *Ceramic Engineering and Science Proceedings*, **21**, 47(2000).
7. M.-C. Shin, J.-S. Cha, J.-H. Lee, S.-H. Lee and H.-S. Lee, *Key Eng. Mater.*, **317-318**, 713(2006).
8. Y. M. Jo, R. B. Hutchison and J. A. Raper, *Powder Tech.*, **91**, 55 (1997).
9. T. Barnett, *Filtr. Separat.*, **Mar**., 28 (2000).
10. L. Films, *Filtr. Separat*., **Mar**., 26 (1999).
11. A. Wimmer, J. L. Cialdini and V. Stumpf, *Chemical Fibers International*, **54**, 31 (2004).
12. H. Jizhi, Z. Jianchun, H. Xinmin and G. Yuhai, *Eur. Polym. J.*, **40**, 667 (2004).
13. C. L. Lin and J. D. Miller, *Chem. Eng. J.*, **80**, 221 (2000).
14. P.-K. Park, C.-H. Lee and S. Lee, *Desalination*, **200**, 302 (2006).
15. L. A. Ni, A. B. Yu, G. Q. Lu and T. Howes, *Miner. Eng.*, **19**, 1084 (2006).
16. J. Kocurek and M. Palica, *Powder Technol.*, **159**, 17 (2005).
17. E. Schmidt, *Filtr. Separat.*, **Sep**., 789 (1995).
18. Y. H. Cheung and C. J. Tsai, *Aerosol Sci. Tech.*, **29**, 315 (1998).
19. M. J. Matteson and C. Orr, *Filtration: Principles and practices,* 2nd Ed., Rev. and Expanded, Marcel Dekker Inc: New York (1987).
20. X. Guangwen, G. Wei and L. Jinghai, *Enginerring Chemistry & Metallurgy (China)*, **17**, 157 (1996).
21. O. Molerus, M. H. Pahl and H. Rumpf, *Chem-Ing-Tech*., **42**, 376 (1971).
22. J. F. Chen, Y. H. Wang, F. Guo, X. M. Wang and C. Zheng, *Ind. Eng. Chem. Res.*, **39**, 948 (2000).
23. C. B. Song, H. S. Park and K. W. Lee, *Powder Technol*., **163**, 152 (2006).